

# Scavenger receptor class B type I (SR-BI) regulates perivascular macrophages and modifies amyloid pathology in an Alzheimer mouse model

Kalliopi Thanopoulou<sup>a</sup>, Apostolia Fragkouli<sup>b</sup>, Fotini Stylianopoulou<sup>c</sup>, and Spiros Georgopoulos<sup>a,1</sup>

<sup>a</sup>Department of Cell Biology, Biomedical Research Foundation, Academy of Athens, 115 27 Athens, Greece; <sup>b</sup>Institute of Biology, National Center for Scientific Research Demokritos, 153 10 Athens, Greece; and <sup>c</sup>Faculty of Nursing, School of Health Sciences, University of Athens, 115 27 Athens, Greece

Edited by Thomas C. Südhof, Stanford University School of Medicine, Palo Alto, CA, and approved October 20, 2010 (received for review May 7, 2010)

Scavenger receptor class B type I (SR-BI) is a high-density lipoprotein receptor that regulates cholesterol efflux from the peripheral tissues to the liver. SR-BI has been identified on astrocytes and vascular smooth muscle cells in Alzheimer's disease brain and has been shown to mediate adhesion of microglia to fibrillar amyloid- $\beta$  (A $\beta$ ). Here we report that SR-BI mediates perivascular macrophage response and regulates A $\beta$ -related pathology and cerebral amyloid angiopathy in an Alzheimer's mouse model. Reduction or deletion of *SR-BI* gene in heterozygous or homozygous deficient mice (*SR-BI*<sup>+/-</sup>, <sup>-/-</sup>) resulted in a significant increase in perivascular macrophages in the brain. SR-BI deletion had no effect on apolipoprotein E or apolipoprotein AI levels in the mouse brain. Our analysis revealed increased levels of SR-BI expression in the brains of human amyloid precursor protein (Swedish, Indiana) transgenic mice (J20 line). To evaluate the role of SR-BI in Alzheimer's disease pathogenesis, we inactivated one *SR-BI* allele in J20 transgenic mice. SR-BI reduction in J20/*SR-BI*<sup>+/-</sup> mice enhanced fibrillar amyloid deposition and cerebral amyloid angiopathy and also exacerbated learning and memory deficits compared with J20 littermates. Immunohistochemical analysis revealed localization of SR-BI on perivascular macrophages in tight association with A $\beta$  deposits. Our data suggest that SR-BI reduction impairs the response of perivascular macrophages to A $\beta$  and enhances the A $\beta$ -related phenotype and cerebral amyloid angiopathy in J20 mice. These results reveal that SR-BI, a scavenger receptor primarily involved in high-density lipoprotein cholesterol transport, plays an essential role in Alzheimer's disease and cerebral amyloid angiopathy.

high-density lipoprotein receptor | dementia

Alzheimer's disease (AD), the major cause of dementia, is a progressive neurodegenerative disease that impairs basic cognitive functions, primarily memory (1). Cerebral amyloid angiopathy (CAA), also characterized by the deposition of amyloid- $\beta$  (A $\beta$ ) in cerebral blood vessels, is common in AD patients (2). Scavenger receptors were originally described for their ability to recognize a broad array of ligands, including lipoproteins (3, 4). Studies using genetically modified mice have established their role in cholesterol metabolism and cardiovascular disease (5, 6). Recently, scavenger receptors have been implicated in AD, although it is unclear whether they contribute to the pathogenesis of the disease (7–10). Scavenger receptor class B type I (SR-BI) has been identified as a high-density lipoprotein (HDL) receptor that mediates cholesterol transport (11). SR-BI has been detected in mouse brain (12), and *SR-BI* gene deletion in mice results in elevated HDL cholesterol and female sterility (5, 13). SR-BI and ATP-binding cassette transporter-1 (ABCA1) play a major role in "reverse cholesterol transport," the HDL-mediated transport of cholesterol from the periphery to the liver (14). ABCA1 has been shown to modulate amyloid plaque formation and apolipoprotein E (ApoE) levels in the brain of Alzheimer's transgenic mice (15). ApoE, a major risk factor for AD (16, 17), is involved in cholesterol homeostasis. Studies have suggested a potential role of SR-BI in AD pathogenesis. SR-BI has been identified on astrocytes in AD brain and on brain macrophages, microglia, and vascular

smooth muscle cells (10, 12). SR-BI-transfected cells internalize aggregates of A $\beta$ , and there is evidence suggesting that SR-BI is able to mediate microglial adhesion to fibrillar A $\beta$  (7, 9). Genetic analysis of AD patients has identified polymorphisms at the genetic locus on chromosome 12, where SR-BI resides (18). Macrophages have been implicated in AD pathogenesis; nevertheless, their role still remains obscure. Macrophages have been shown to degrade A $\beta$  in vitro (19) and bone-marrow-derived perivascular macrophages have also been implicated in AD, as they can remove A $\beta$  peptides from brain vessels and regulate CAA (20, 21).

In this study, we examine the role of SR-BI in the development of the amyloid-related phenotype and CAA in a human amyloid precursor protein (huAPP) (Swedish, Indiana) transgenic mouse (J20 line). We show that SR-BI regulates perivascular macrophages in the mouse brain. Reduction or deletion of *SR-BI* in heterozygous and homozygous mice caused a significant increase in perivascular macrophages. Inactivation of a single *SR-BI* allele resulted in reduction of SR-BI protein approximately by half in the brain, as has previously been reported for the expression of SR-BI in the liver of heterozygous mice (5). Analysis of SR-BI expression in J20 mouse brains showed elevated SR-BI protein levels compared with wild-type littermates. To evaluate the role of SR-BI in AD, we generated J20/*SR-BI* heterozygous knockout mice (*SR-BI*<sup>+/-</sup>) by mating J20 mice with *SR-BI* heterozygous knockout mice (5, 22). Analysis of 11-mo-old J20/*SR-BI*<sup>+/-</sup> mice revealed a significant increase in amyloid plaque formation and vascular amyloid deposition in the brain and exacerbated learning and memory deficits compared with their J20 littermates. Our findings suggest that inactivation of a single *SR-BI* allele is sufficient to impair perivascular macrophage response to A $\beta$  and to enhance fibrillar amyloid deposition and CAA.

## Results

**Generation of J20/*SR-BI*<sup>+/-</sup> Mice.** J20 male mice were mated with *SR-BI*<sup>+/-</sup> female mice. We used heterozygous mice, as *SR-BI* female homozygous mutant mice are sterile (13). Probuconol has been shown to reverse the infertility problems of *SR-BI* mutant mice (13), nevertheless we decided not to use it as it has been shown to increase ApoE levels in the brain (23) that could possibly affect the phenotype of the mice. We attempted to generate J20 mice that were *SR-BI* homozygote deficient (J20/*SR-BI*<sup>-/-</sup>) by mating J20/*SR-BI*<sup>+/-</sup> male mice with *SR-BI*<sup>+/-</sup> female mice. In the offspring, we identified only J20/*SR-BI*<sup>+/-</sup> and not any J20/*SR-BI*<sup>-/-</sup> mice. We believe that the combination of the fertility problems of the *SR-BI* female mice with the increased mortality and fertility problems observed in mice expressing high levels

Author contributions: S.G. designed research; K.T. and A.F. performed research; F.S. contributed new reagents/analytic tools; K.T., A.F., and S.G. analyzed data; and S.G. wrote the paper.

The authors declare no conflict of interest.

This article is a PNAS Direct Submission.

<sup>1</sup>To whom correspondence should be addressed. E-mail: sgeorgopoulos@bioacademy.gr.

This article contains supporting information online at [www.pnas.org/lookup/suppl/doi:10.1073/pnas.1005888107/-DCSupplemental](http://www.pnas.org/lookup/suppl/doi:10.1073/pnas.1005888107/-DCSupplemental).

of huAPP including J20 (24) hindered the generation of J20/*SR-BI*<sup>-/-</sup> mice. However, we cannot exclude the possibility that this was an effect caused by the absence of SR-BI combined with the expression of huA $\beta$ .

**SR-BI Expression Is Increased in J20 Mouse Brains.** SR-BI has been identified in the human AD brain and in normal mouse brain (12, 25). To evaluate the involvement of SR-BI in the AD phenotype of J20 mice, we examined for possible changes in the expression levels of SR-BI in the brains of J20 mice. Analysis of total protein brain extracts of 11-mo-old mice by Western blotting showed a significant increase in SR-BI levels in J20 mouse brains (Fig. 1A) ( $n = 4-5$ ) (wild-type versus J20,  $P = 0.0072$ ). This result clearly suggests the involvement of SR-BI in the AD pathology in J20 mice.

**SR-BI Reduction Increases Perivascular Macrophages in the Mouse Brain.** Previous analysis of liver protein extracts of *SR-BI*<sup>+/-</sup> mice revealed a reduction in SR-BI protein approximately by half in heterozygous mutants compared with wild-type (5). To examine the effect of inactivation of one SR-BI allele in the brain, we analyzed brain protein extracts by Western blotting. Our results showed a reduction approximately by half in SR-BI protein levels in heterozygous brains (Fig. S1) ( $n = 3-5$ ) (one-way ANOVA,  $P = 0.0276$ ). To evaluate the impact of SR-BI reduction in perivascular macrophages in the mouse brain, we analyzed the expression of CD206 and CD163 in *SR-BI*<sup>+/-</sup> and <sup>-/-</sup> mice. CD206, a mannose receptor, and CD163, a scavenger receptor, have been identified as perivascular macrophage markers (26, 27). Analysis of total protein brain extracts by Western blotting showed a significant increase in both CD206 and CD163 in *SR-BI*<sup>+/-</sup> and <sup>-/-</sup> mice compared with wild-type mice ( $n = 5$ ) (CD206 wild-type versus *SR-BI*<sup>+/-</sup>,  $P = 0.0446$ ; wild-type versus *SR-BI*<sup>-/-</sup>,  $P = 0.0018$ ; CD163 wild-type versus *SR-BI*<sup>+/-</sup>,  $P = 0.0467$ ; wild-type versus *SR-BI*<sup>-/-</sup>,  $P = 0.0064$ ; Fig. 1B). The same effect was observed when brain sections from *SR-BI*<sup>+/-</sup> and wild-type mice were immunostained with a CD206-specific antibody, where *SR-BI*<sup>+/-</sup> brain sections exhibited a more intense staining compared with wild-type (Fig. 1C) ( $n = 4$ ) (wild-type versus *SR-BI*<sup>+/-</sup>,  $P = 0.0445$ ). We next examined CD206 levels by Western blotting from wild-type, J20, *SR-BI*<sup>+/-</sup>, and J20/*SR-BI*<sup>+/-</sup> mice. We found a significant increase in the J20 mice compared with the wild-type mice. Comparison of CD206 levels between the J20/*SR-BI*<sup>+/-</sup> and the *SR-BI*<sup>+/-</sup> mice also showed a significant increase that was twofold the increase between wild-type and J20 mice (Fig. 1D) ( $n = 4-5$ ) (wild-type versus J20,  $P = 0.0452$ ; J20 versus J20/*SR-BI*<sup>+/-</sup>,  $P = 0.00169$ ; *SR-BI*<sup>+/-</sup> versus J20/*SR-BI*<sup>+/-</sup>,  $P = 0.0183$ ). Our results clearly support that SR-BI protein levels have a direct effect on the perivascular macrophage and suggest that this increase compensates for the loss of SR-BI.

**SR-BI Reduction in the Brain of J20/*SR-BI*<sup>+/-</sup> Mice Accelerates Cerebrovascular and Parenchymal Amyloid Plaque Formation.** Brains of 11-mo-old J20 and J20/*SR-BI*<sup>+/-</sup> mice ( $n = 12$ ) were analyzed for vascular and parenchymal amyloid deposits with thioflavine-S. In all J20/*SR-BI*<sup>+/-</sup> brains examined, blood vessels in the hippocampus (Fig. 2B) and the cortex (Fig. 2D) contained large thioflavin-S-positive deposits with a characteristic pattern of amyloid deposition in concentric rings (Fig. 2B). J20 littermates also exhibited vascular deposits positive for thioflavine-S but to a much lesser extent (Fig. 2A and C). Densitometric analysis of vascular thioflavine-S deposition revealed a significant increase in J20/*SR-BI*<sup>+/-</sup> brains (Fig. 2E) ( $P = 0.0273$ ). We next examined for parenchymal amyloid deposition in the brains of the mice. In both groups, the majority of thioflavine-S-positive deposits were predominantly localized in the hippocampus, with a few plaques in the cortex (Fig. 2F and G). Our analysis revealed a statistically significant increase in thioflavine-S-positive plaques in the hippocampi of J20/*SR-BI*<sup>+/-</sup> mice compared with J20 (Fig. 2H) ( $P = 0.0190$ ). No obvious differences were observed in the anatomical distribution or the staining pattern of the plaques between the two groups. To determine differences in am-

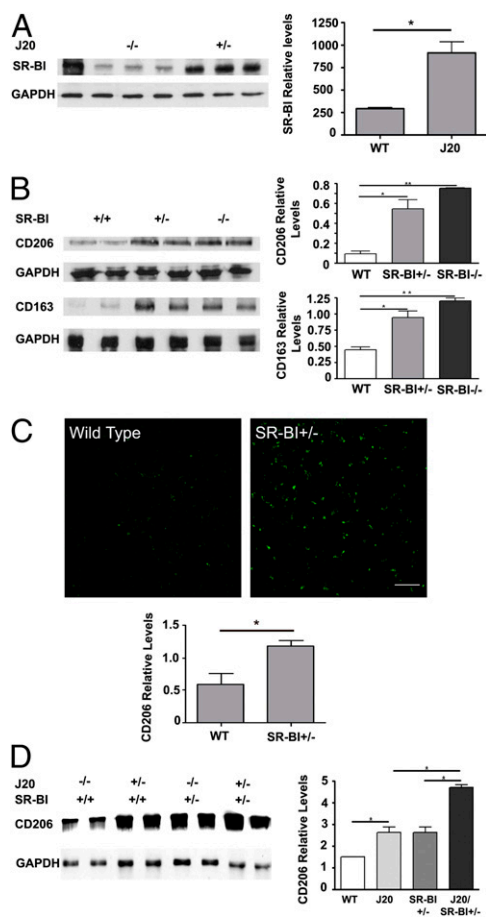


**Fig. 1.** J20 mouse brains have increased SR-BI protein levels, and *SR-BI* reduction or deletion increases perivascular macrophages in the mouse brain. (A) Western and densitometric analysis of brain lysates of wild-type and J20 revealed a significant increase in SR-BI protein in J20 brains. First lane is wild-type liver lysate as positive control ( $*P < 0.01$ ). (B) Western and densitometric analysis of brain lysates of *SR-BI*<sup>+/+</sup>, <sup>+/-</sup>, and <sup>-/-</sup> mice revealed a significant increase in CD206 and CD163 ( $*P < 0.05$ ;  $**P < 0.01$ ). (C) Representative images and densitometric analysis of cortex immunostained for CD206 depicting strong immunoreactivity in the *SR-BI*<sup>+/-</sup> brain ( $*P < 0.05$ ). (Scale bar, 10  $\mu$ m.) (D) Western and densitometric analysis of brain lysates of *SR-BI*<sup>+/+</sup>, J20/*SR-BI*<sup>+/+</sup>, *SR-BI*<sup>+/-</sup>, and J20/*SR-BI*<sup>+/-</sup> mice showed increased CD206 levels for J20 and J20/*SR-BI*<sup>+/-</sup> mice ( $*P < 0.05$ ). Protein levels were standardized with GAPDH. Western blots show two representative samples per group. Values represent mean  $\pm$  SEM of samples.

ylod deposition, we immunostained brain sections of the same animals using an A $\beta$ -specific antibody (Fig. 2I and J). Strong A $\beta$  staining was observed in both groups, nevertheless quantitation did not reveal any significant difference between them (Fig. 2K). Next we analyzed the insoluble (guanidine fraction) and soluble (lysis fraction) A $\beta$ <sub>40</sub> and A $\beta$ <sub>42</sub> levels by ELISA between J20 and J20/*SR-BI*<sup>+/-</sup> mice, where we noticed a small but nonsignificant increase in A $\beta$ <sub>42</sub> levels in the guanidine extract of J20/*SR-BI*<sup>+/-</sup> brains (Fig. S2). These results suggest that SR-BI reduction clearly promotes fibrillar A $\beta$  formation, with the brain vasculature being more affected.

**ApoE and ApoAI Levels in the Mouse Brain Are Not Affected by SR-BI.** To evaluate for possible changes in ApoE and ApoAI in the mouse brain, we examined by Western blotting total protein brain extracts of *SR-BI*<sup>+/+</sup>, <sup>+/-</sup>, and <sup>-/-</sup> mice. Our analysis showed no differences in ApoE (Fig. S3A) or ApoAI (Fig. S4). To further examine the effects of SR-BI reduction on ApoE expression in the J20 and J20/*SR-BI*<sup>+/-</sup> brains, we analyzed by Western blotting different fractions of brain extracts (PBS/lysis/

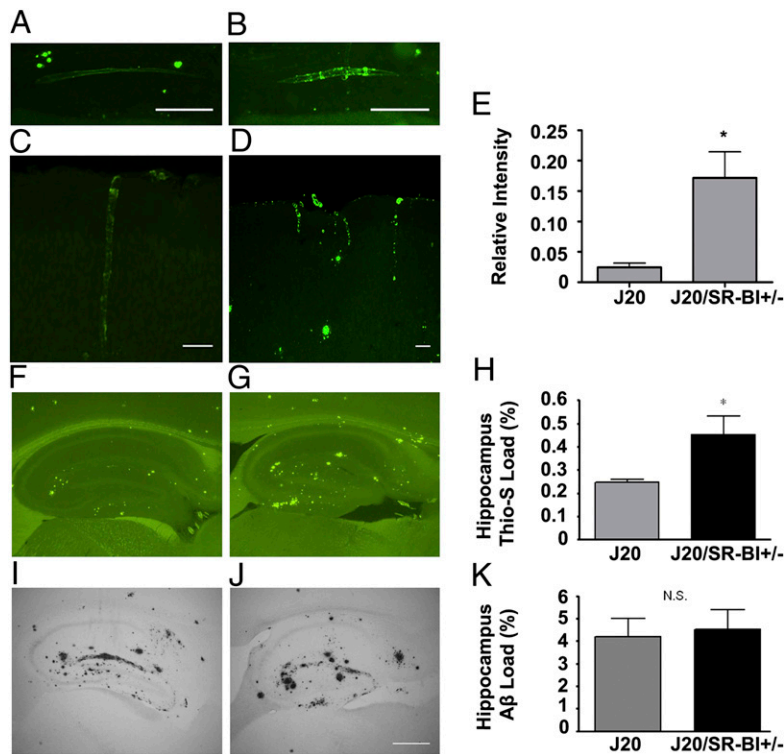


**Fig. 2.** SR-BI reduction increases vascular and hippocampal fibrillar amyloid deposition in the mouse brain. (A and B) Sagittal sections of hippocampus from J20 and J20/SR-BI<sup>+/-</sup> mice showing amyloid deposition in vessel walls. (C and D) Amyloid deposition in cortical vessels in J20 and J20/SR-BI<sup>+/-</sup> mice. (Scale bars, 10  $\mu$ m.) (E) Densitometric analysis of vascular thioflavine-S load revealed increased vascular fibrillar A $\beta$  deposition in J20/SR-BI<sup>+/-</sup> mice (\* $P$  < 0.05). (F and G) Sagittal sections of 11-mo-old J20 and J20/SR-BI<sup>+/-</sup> hippocampi stained with thioflavine-S or immunostained with an anti-A $\beta$  antibody (I and J). (Scale bar, 200  $\mu$ m.) (H and K) Percent area covered by thioflavine-S fluorescence (\* $P$  < 0.05,  $n$  = 12) (H) or A $\beta$  staining [ $P$  = N.S. (nonsignificant),  $n$  = 12] (K) were quantified in the hippocampus, showing a significant increase in thioflavine-S-positive amyloid deposits.

guanidine fractions), where we found no significant differences in ApoE (Fig. S3B). Our results showed that SR-BI reduction did not have any effect on the expression levels of ApoE either in the non-huAPP or the huAPP transgenic brains.

**SR-BI Is Located on Perivascular Macrophages and Colocalizes with A $\beta$ .** Immunostaining for SR-BI and CD206 in wild-type brain showed colocalization that demonstrates the presence of SR-BI on perivascular macrophages in capillary blood vessels in the meninges (Fig. 3E) and in the brain parenchyma (Fig. 3F). Next we stained brain sections of J20 mice for SR-BI and A $\beta$  to examine the association between SR-BI and A $\beta$ . We used an SR-BI-specific antibody together with an A $\beta$ -specific antibody (6E10) that stains A $\beta$  in diffuse amyloid plaques (Fig. 3A and B) or thioflavine-S that stains fibrillar A $\beta$  in compact amyloid plaques (Fig. 3C and D). Our analysis showed that SR-BI is in tight association with A $\beta$  deposits in meningeal (Fig. 3A) and cortical capillary vessels (Fig. 3B) and colocalizes with thioflavine-S-positive meningeal vessels (Fig. 3C). In some cases, we could clearly distinguish a layer of A $\beta$  surrounded by CD206 in cortical and meningeal blood vessels (Fig. 3A). There was strong expression of SR-BI in the blood vessels close to amyloid deposits (Fig. 3D). Our results show colocalization of SR-BI with fibrillar A $\beta$  and CD206 that implies the involvement of SR-BI and perivascular macrophages in A $\beta$  clearance.

**SR-BI Reduction Has No Effect on the Capacity of Peripheral Macrophages and Microglia to Phagocytose A $\beta$ .** To evaluate the effect of SR-BI reduction in the phagocytic activity of peripheral macrophages and microglia toward A $\beta$ , we analyzed A $\beta$  phagocytosis by peripheral macrophages and neonatal microglia from SR-BI<sup>+/-</sup> and wild-type adult mice and newborn pups, respectively. Confocal microscopic analysis clearly revealed microglial and peripheral macrophages containing FITC-labeled A $\beta$  in SR-BI<sup>+/-</sup> and wild-type cells. Quantitation analysis showed no significant differences in A $\beta$  phagocytosis between SR-BI<sup>+/-</sup> and wild-type for both the microglial and the peripheral macrophage cultures (Fig. S5). This result implies that SR-BI reduction does not have an obvious effect on the capacity of these cell types to phagocytose A $\beta$ .

**SR-BI Reduction Has No Effect on Astrocytes and Microglia.** To evaluate the role of SR-BI in reactive astrocytes and activated microglial cells in amyloid deposition, we examined brain sections from J20 and J20/SR-BI<sup>+/-</sup> mice. We located Iba-1-positive microglia and glial fibrillary acidic protein (GFAP)-positive astrocytes surrounding thioflavine-S-positive amyloid plaques. We did not observe any significant differences between the two groups (Fig. S6A and B).

**SR-BI Reduction Has No Effect on Oxidative Stress and APP Processing.** Oxidative damage and mitochondrial dysfunction have been implicated in the pathogenesis of AD. Brains from SR-BI<sup>+/+</sup> and <sup>+/-</sup> mice were analyzed by Western blotting for superoxide dismutase-2 (SOD2) protein levels, a marker of oxidative stress. No significant difference was observed (Fig. S7A). In addition, we analyzed total brain extracts of J20 and J20/SR-BI<sup>+/-</sup> mice, where again there was no obvious difference between the two groups (Fig. S7B). To examine whether the reduction of SR-BI affects APP processing, we examined the levels of cell-associated carboxy-terminal fragments (CTF $\alpha$  and CTF $\beta$ ) as well as the amount of full-length APP protein of total brain extracts of J20 and J20/SR-BI<sup>+/-</sup> mice by Western blotting. There was no difference between J20 and J20/SR-BI<sup>+/-</sup> mice. These results demonstrate that reduction of SR-BI did not affect APP processing (Fig. S7C).

**SR-BI Reduction Accelerates Behavioral Deficits in huAPP Mice.** To evaluate whether SR-BI reduction worsened the cognitive deficits, we compared the behavior of huAPP/SR-BI<sup>+/-</sup> and huAPP mice as opposed to wild-type controls in open-field, novel object recognition, and water-maze tests. In the open field, no statistically significant difference was observed in horizontal (crosses) or vertical (rears) activity among the groups (Fig. 4A and B). No difference in activity was found either on the first day of testing in a novel environment (crosses: one-way ANOVA:  $F_{(2,21)} = 0.300$ ,  $P = 0.744$ ; rears: one-way ANOVA:  $F_{(2,21)} = 0.869$ ,  $P = 0.902$ ) or on the second day of testing in a more familiar environment (crosses: one-way ANOVA:  $F_{(2,21)} = 0.104$ ,  $P = 0.902$ ; rears: one-way ANOVA:  $F_{(2,21)} = 0.590$ ,  $P = 0.565$ ). To evaluate proper recognition memory, we used the novel object recognition task (28). All animals subjected to this task were able to discriminate

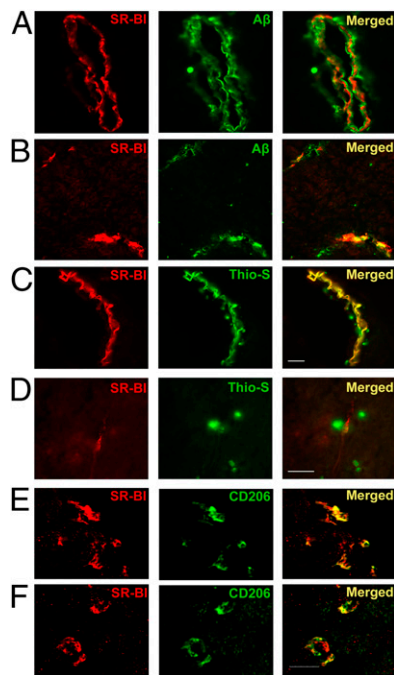


**Fig. 3.** SR-BI is in tight association with A $\beta$  and colocalizes with CD206. (A and B) Immunostaining for SR-BI and A $\beta$ . (A) Meningeal blood vessel showing a layer of A $\beta$  coated with SR-BI. (B) Cortical blood vessels showing colocalization of SR-BI and A $\beta$ . (C and D) Immunostaining for SR-BI and thioflavine-S-positive amyloid deposition. (C) Meningeal blood vessel showing colocalization between SR-BI and thioflavine-S-positive amyloid deposits. (Scale bars for A–C, 30  $\mu$ m.) (D) Thioflavine-S-positive amyloid plaques extending toward an SR-BI-positive cortical blood vessel. (Scale bar, 30  $\mu$ m.) (E and F) Immunofluorescence staining for SR-BI and CD206 in the meninges (E) and in the cortex (F) of wild-type mouse brain shows colocalization. (Scale bars for E and F, 50  $\mu$ m.)

between the familiar and the novel objects. Nevertheless, when the discrimination ratio was examined, a statistically significant effect of genotype was observed (Fig. 4C) (discrimination ratio: one-way ANOVA:  $F_{(2,1)} = 6.495$ ,  $P = 0.007$ ). Post hoc analysis revealed that huAPP/SR-BI<sup>+/-</sup> mice performed worse on this task compared with their wild-type and huAPP littermates. Hippocampus-dependent spatial learning was also examined, using the water-maze task (29). Irrespective of their genotype, all mice used in this task appeared to swim normally and had no difficulty in mounting the platform provided. Furthermore, when the escape platform was marked with a visible cue, all mice learned to approach it directly and gradually reduced their latency across the 3-d training period (Fig. 4D) (time required to reach the escape platform: ANOVA repeated measures:  $F_{(2,19)} = 1.734$ ,  $P = 0.203$ ). After training with the visible platform, mice were tested in the hidden-platform version of the water-maze task and latency to reach the hidden platform was used as a parameter of learning. Compared with their wild-type littermates, both J20 and J20/SR-BI<sup>+/-</sup> mice took longer to find the hidden platform (Fig. 4D) (ANOVA for repeated measures:  $F_{(2,19)} = 19.551$ ,  $P < 0.001$  and Bonferroni post hoc analysis). Interestingly, J20/SR-BI<sup>+/-</sup> mice appeared to perform worse in this task compared with the two other mouse groups (Fig. 4D) (Bonferroni post hoc analysis). Finally, when swim speed was examined, no difference was observed among mice of different genotype (wild-type: 16.3 cm/s  $\pm$  1.3; J20: 16.6 cm/s  $\pm$  2; J20/SR-BI = 12.3 cm/s  $\pm$  1.3; one-way ANOVA:  $F_{(2,21)} = 2.685$ ,  $P = 0.094$ ). In the probe trial, only wild-type mice displayed a preference for the target quadrant, and spent more than 30% of their time in this quadrant. Our statistical analysis revealed a genotype effect on time spent both in the target and opposite quadrants (Fig. 4E) (target: one-way ANOVA:  $F_{(2,21)} = 9.608$ ,  $P = 0.001$ ; opposite: one-way ANOVA:  $F_{(2,21)} = 6.694$ ,  $P = 0.006$ ). Compared with

wild-type controls, both J20 and J20/SR-BI<sup>+/-</sup> mice spent less time in the target (Bonferroni post hoc analysis), whereas only J20/SR-BI<sup>+/-</sup> mice spent more time in the opposite one (Fig. 4E) (post hoc analysis). Representative paths followed by animals of different groups are shown in Fig. 4F.

## Discussion

In this study, we focused on the role of SR-BI in the development of the AD-like phenotype in huAPP transgenic mice (J20). We show that SR-BI expression is distinctively elevated in the J20 mouse brains. Inactivation of a single SR-BI allele is sufficient to promote a significant increase in fibrillar A $\beta$  vascular deposition and fibrillar amyloid plaque formation in the brain as well as to exacerbate A $\beta$ -dependent behavioral abnormalities. We suggest that this phenotype results from the reduction of SR-BI in the brain. We propose that this effect is mediated primarily by perivascular macrophages, as SR-BI reduction causes a significant increase in perivascular macrophages in the brain.

In this study, we demonstrate that SR-BI is clearly associated with perivascular macrophages. Perivascular macrophages are bone-marrow-derived innate immune cells (30). They have been implicated in CNS inflammation and more recently in AD (21). To identify perivascular macrophages, we used CD163, a hemoglobin-haptoglobin scavenger receptor, and CD206, a mannose receptor (20, 26, 27). Analysis of SR-BI mutant mice revealed a remarkable increase in CD206 and CD163 in the brain. This was confirmed both for homozygous and the heterozygous SR-BI mice, implying that reduction of SR-BI is sufficient to trigger this effect. We hypothesize that the increase in perivascular macrophages compensates for the loss of SR-BI. Next we examined CD206 expression in the brains of J20 mice, where it was elevated. We suggest that this is due to the recruitment of perivascular macrophages to A $\beta$ . To evaluate the effect of SR-BI reduction in the response of perivascular macrophages to A $\beta$ , we compared CD206 expression between J20/SR-BI<sup>+/-</sup> and control SR-BI<sup>+/-</sup> mouse brains. We observed a significant increase in CD206 levels in J20/SR-BI<sup>+/-</sup> brains, which was approximately twofold the increase in CD206 we observed between wild-type and J20 mice. The latter finding suggests that in the J20/SR-BI<sup>+/-</sup> mice the increase in perivascular macrophages compensates for the reduction of SR-BI. Our data imply that SR-BI plays a major role in the response of perivascular macrophages to A $\beta$  and that reduction of SR-BI impairs this response.

In our study, we used J20 mice that develop amyloidosis and cerebrovascular pathology (22, 31). Analysis for fibrillar amyloid deposition revealed a significant increase in vascular amyloid deposits and in the fibrillar amyloid plaques in the hippocampus in J20/SR-BI<sup>+/-</sup> mice. More prominent was the effect on the fibrillar amyloid deposition in J20/SR-BI<sup>+/-</sup> mice. Given that SR-BI is located on perivascular macrophages in the brain vessels, it is possible that the increase of the fibrillar amyloid deposits in J20/SR-BI<sup>+/-</sup> mice in the brain parenchyma can be attributed to the incapacity of the vasculature to clear A $\beta$ .

Previous work has suggested that eliminating perivascular macrophages can bring an increase in A $\beta_{42}$  levels in the vasculature and a decrease in the cortex parenchyma (20). This effect is more likely to reflect a redistribution of A $\beta$  in blood vessels and brain parenchyma rather than a substantial change in total A $\beta$  levels in the brain. Our analysis revealed a small but nonsignificant increase in A $\beta_{42}$  levels between J20 and J20/SR-BI<sup>+/-</sup>, as it was done on total brain protein extracts that included the vasculature and brain parenchyma. Immunohistochemical analysis of brain sections for A $\beta$  deposition showed no significant differences as well.

To evaluate the effect of SR-BI deletion on ApoE in the mouse brain, we analyzed ApoE expression in SR-BI<sup>+/+</sup>, <sup>+/-</sup>, and <sup>-/-</sup> mice without detecting any differences. This was anticipated, as SR-BI deletion in mutant mice has been shown to have no effect on ApoE (6). To investigate for any relevance between the increase in amyloid deposition and ApoE, we compared ApoE levels in J20/SR-BI<sup>+/-</sup> and J20 brains, where we again found no differences. Because SR-BI deletion up-regulates ApoAI in

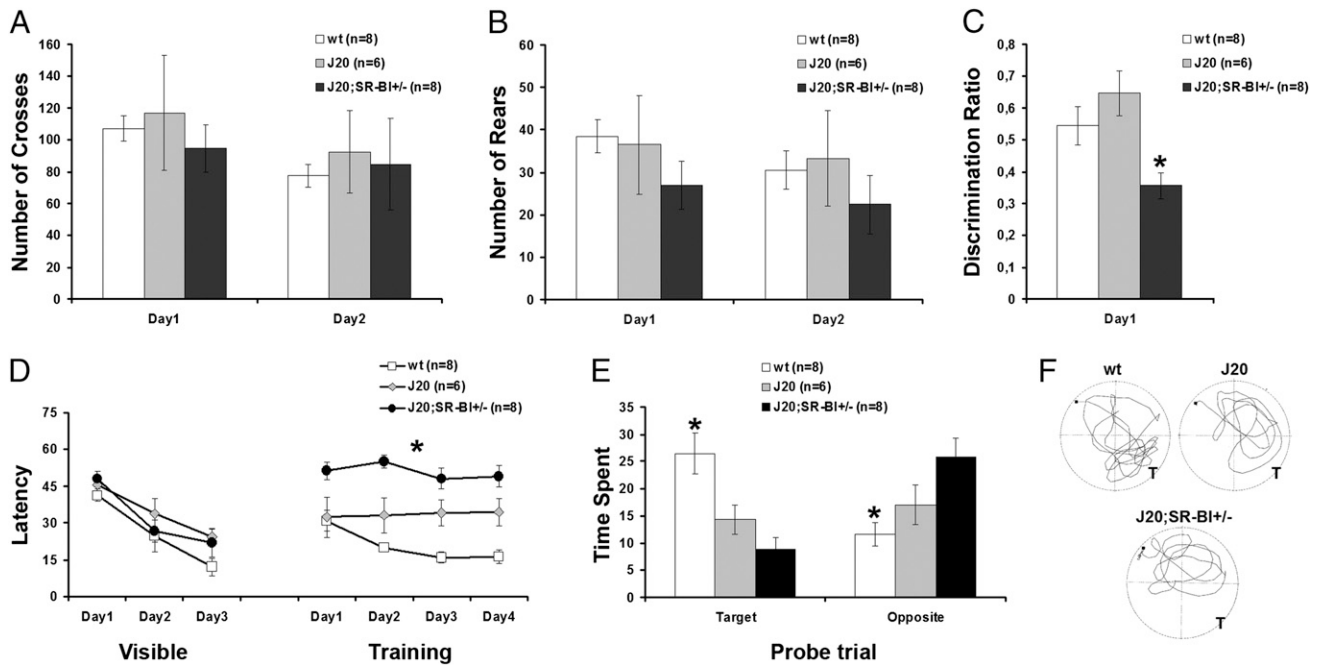


**Fig. 4.** Reduction of SR-BI exacerbated learning and memory deficits, but not motor skills, of J20 animals. (A and B) Performance in the open field. (A) Horizontal activity was assessed by scoring cross-overs in the open field (data points depict mean  $\pm$  SEM); no difference was observed among the animal groups examined in both a novel (first day of testing) and a familiar (second day of testing) environment. (B) Vertical activity was assessed by scoring rears in the open field (data points depict mean  $\pm$  SEM); no difference was observed among the animals in either the first or second day of testing. (C) Mean discrimination ratio ( $\pm$  SEM) in the novel object recognition task. All animals were able to discriminate between the novel and the familiar object. Interestingly, J20/SR-BI<sup>+/-</sup> mice perform worse in this task. (D–F) Performance in the water-maze task. (D) Mean latency ( $\pm$  SEM) across visible and training sessions of the water maze. No difference was observed in the latency to reach a visible platform. In the training session, J20/SR-BI<sup>+/-</sup> mice perform worse compared with the other two mouse groups. (E) Mean time spent ( $\pm$  SEM) in the target and the opposite quadrants of the water maze during the probe trial. In the absence of the escape platform, wild-type animals showed a preference for the target quadrant. J20/SR-BI<sup>+/-</sup> mice spent significantly more time in the more distant (opposite) quadrant compared with the other two groups. (F) Representative paths followed by mice of each group during the probe trial. T, target. \* $P < 0.05$ .

the periphery (6), we asked whether reduction of SR-BI would have any impact on ApoAI in the mouse brain. Our analysis on SR-BI<sup>+/+</sup>, <sup>+/-</sup>, and <sup>-/-</sup> brains showed no differences in ApoAI levels. In conclusion, our results demonstrate that ApoE and ApoAI are not affected by SR-BI in the mouse brain and suggest that the effects of SR-BI on amyloid deposition are independent of ApoE.

In a similar study, detection of perivascular macrophages with CD206 confirmed colocalization with fibrillar amyloid deposits (20). Our results revealed colocalization of SR-BI with CD206 and fibrillar A $\beta$  on meningeal and cortical vessels. We observed SR-BI in tight association with amyloid deposits in the blood vessels. Interestingly, we noticed persistent and intense SR-BI staining in blood vessels in close vicinity of parenchymal fibrillar amyloid plaques.

Although SR-BI has been detected in astrocytes in the human AD brain (12), we observed SR-BI staining primarily located in the blood vessels in the mouse brain. Immunohistochemical analysis for GFAP and Iba-1 immunoreactivity did not reveal any significant differences, demonstrating that SR-BI reduction did not affect astrocytic or microglial response to A $\beta$ . Our data are in agreement with previous findings where inhibition of SR-BI–A $\beta$  interactions with a blocking antibody to SR-BI did not affect binding of A $\beta$  by astrocytes and suggest a limited role for SR-BI in the interaction of mouse astrocytes with A $\beta$  (32). Moreover, we showed that SR-BI reduction has little effect on the capacity of peripheral macrophage and microglial cell cultures to bind labeled A $\beta$ , indicating that the effect on amyloid deposition by SR-BI is mediated primarily by perivascular macrophages.

SR-BI deletion promotes a significant increase in oxidative stress markers in the blood serum in SR-BI knockout mice (33). J20 mice have been shown to have increased production of superoxide (O<sub>2</sub><sup>-</sup>) and elevated levels of superoxide dismutase-2

(SOD2) (34). Analysis of SOD2 expression in SR-BI<sup>+/+</sup> and <sup>+/-</sup> mice as well as in J20/SR-BI<sup>+/-</sup> and J20 showed no changes, implying that SR-BI does not affect oxidative stress in the brain.

In addition to the histopathological findings, behavioral and memory analysis of J20/SR-BI<sup>+/-</sup> mice clearly revealed further cognitive impairment compared with J20 littermates. HuAPP mice have been shown to have a range of behavioral alterations and memory deficits (35). SR-BI homozygous deficient mice, on the other hand, are normal on a variety of behavioral tests, including open field, novel object recognition, and water maze, at all ages with the exception of very old (20- to 26-mo-old) homozygous mice, which have impaired long-term potentiation (LTP) (36). In our experiments, we used 11-mo-old mice that were heterozygous knockout for SR-BI. Our behavioral data showing exacerbated learning and memory deficits in J20/SR-BI<sup>+/-</sup> mice support our histopathological findings and confirm the essential role of SR-BI in the development of the AD phenotype in J20 mice.

Our study links SR-BI to perivascular macrophages and establishes a significant role for SR-BI among other scavenger receptors in AD and CAA (37). Our work supports the hypothesis that SR-BI is involved in amyloid pathology primarily as a modulator of the perivascular macrophage response. Activation of the peripheral immune cells through receptors of the innate immune system, such as the TLR9, has been shown to reduce AD-related pathology and CAA in AD mouse models (38). Similarly, SR-BI activation could possibly have a beneficial effect in AD pathology. SR-BI expression has been shown to be induced by statins (39, 40), and simvastatin treatment of J20 mice has shown a positive effect on cerebrovascular function (34). These data combined with ours suggest SR-BI as a potential mediator of the beneficial effect of statins in cerebrovascular function. Our study relates SR-BI with perivascular macrophages and demonstrates a significant role for

SR-BI in CAA and AD. These findings could possibly have major implications for the treatment of AD and CAA and designate SR-BI as a therapeutical target.

## Methods

**Animals.** All animal procedures were approved by the Bioethical Committee of the Biomedical Research Institute. All animal experiments were in agreement with ethical recommendations of the European Communities Council Directive (86/609/EEC). J20 transgenic and SR-BI mice were on C57Bl6/J background.

**Immunohistochemistry.** Vibratome sections were incubated overnight with anti-A $\beta$  biotinylated 6E10 and developed by using 3,3'-diaminobenzidine/nickel. For thioflavine-S plus GFAP/Iba-1/SR-BI double labeling, sections were incubated overnight with anti-GFAP, anti-Iba-1, and anti-SR-BI, exposed to secondary antibodies, and then processed for thioflavine-S staining. Cryosections were incubated overnight with anti-CD206, and developed with an anti-rat FITC antibody. For CD206 plus SR-BI double labeling, sections were incubated overnight with anti-CD206 and then processed for SR-BI.

- Selkoe DJ (1991) The molecular pathology of Alzheimer's disease. *Neuron* 6:487–498.
- Nicoll JA, Yamada M, Frackowiak J, Mazur-Kolecka B, Weller RO (2004) Cerebral amyloid angiopathy plays a direct role in the pathogenesis of Alzheimer's disease. Pro-CAA position statement. *Neurobiol Aging* 25:589–597; discussion 603–604.
- Peiser L, Gordon S (2001) The function of scavenger receptors expressed by macrophages and their role in the regulation of inflammation. *Microbes Infect* 3:149–159.
- Terpstra V, van Amersfoort ES, van Velzen AG, Kuiper J, van Berkel TJ (2000) Hepatic and extrahepatic scavenger receptors: Function in relation to disease. *Arterioscler Thromb Vasc Biol* 20:1860–1872.
- Rigotti A, et al. (1997) A targeted mutation in the murine gene encoding the high density lipoprotein (HDL) receptor scavenger receptor class B type I reveals its key role in HDL metabolism. *Proc Natl Acad Sci USA* 94:12610–12615.
- Varban ML, et al. (1998) Targeted mutation reveals a central role for SR-BI in hepatic selective uptake of high density lipoprotein cholesterol. *Proc Natl Acad Sci USA* 95:4619–4624.
- Paresce DM, Ghosh RN, Maxfield FR (1996) Microglial cells internalize aggregates of the Alzheimer's disease amyloid  $\beta$ -protein via a scavenger receptor. *Neuron* 17:553–565.
- El Khoury J, et al. (1996) Scavenger receptor-mediated adhesion of microglia to  $\beta$ -amyloid fibrils. *Nature* 382:716–719.
- Husemann J, Loike JD, Kodama T, Silverstein SC (2001) Scavenger receptor class B type I (SR-BI) mediates adhesion of neonatal murine microglia to fibrillar  $\beta$ -amyloid. *J Neuroimmunol* 114:142–150.
- Husemann J, Loike JD, Anankov R, Febbraio M, Silverstein SC (2002) Scavenger receptors in neurobiology and neuropathology: Their role on microglia and other cells of the nervous system. *Glia* 40:195–205.
- Steinberg D (1996) A docking receptor for HDL cholesterol esters. *Science* 271:460–461.
- Husemann J, Silverstein SC (2001) Expression of scavenger receptor class B, type I, by astrocytes and vascular smooth muscle cells in normal adult mouse and human brain and in Alzheimer's disease brain. *Am J Pathol* 158:825–832.
- Miettinen HE, Rayburn H, Krieger M (2001) Abnormal lipoprotein metabolism and reversible female infertility in HDL receptor (SR-BI)-deficient mice. *J Clin Invest* 108:1717–1722.
- Rigotti A, Miettinen HE, Krieger M (2003) The role of the high-density lipoprotein receptor SR-BI in the lipid metabolism of endocrine and other tissues. *Endocr Rev* 24:357–387.
- Wahrle SE, et al. (2005) Deletion of Abca1 increases A $\beta$  deposition in the PDAPP transgenic mouse model of Alzheimer disease. *J Biol Chem* 280:43236–43242.
- Kim J, Basak JM, Holtzman DM (2009) The role of apolipoprotein E in Alzheimer's disease. *Neuron* 63:287–303.
- Georgopoulos S, McKee A, Kan HY, Zannis VI (2002) Generation and characterization of two transgenic mouse lines expressing human ApoE2 in neurons and glial cells. *Biochemistry* 41:9293–9301.
- Zubenko GS, Hughes HB, Stiffler JS, Hurtt MR, Kaplan BB (1998) A genome survey for novel Alzheimer disease risk loci: Results at 10-cM resolution. *Genomics* 50:121–128.
- Majumdar A, et al. (2008) Degradation of fibrillar forms of Alzheimer's amyloid  $\beta$ -peptide by macrophages. *Neurobiol Aging* 29:707–715.
- Hawkes CA, McLaurin J (2009) Selective targeting of perivascular macrophages for clearance of  $\beta$ -amyloid in cerebral amyloid angiopathy. *Proc Natl Acad Sci USA* 106:1261–1266.
- Williams K, Alvarez X, Lackner AA (2001) Central nervous system perivascular cells are immunoregulatory cells that connect the CNS with the peripheral immune system. *Glia* 36:156–164.
- Mucke L, et al. (2000) High-level neuronal expression of A $\beta$ <sub>1–42</sub> in wild-type human amyloid protein precursor transgenic mice: Synaptotoxicity without plaque formation. *J Neurosci* 20:4050–4058.
- Champagne D, Pearson D, Dea D, Rochford J, Poirier J (2003) The cholesterol-lowering drug probucol increases apolipoprotein E production in the hippocampus of aged rats: Implications for Alzheimer's disease. *Neuroscience* 121:99–110.
- Chin J, et al. (2005) Fyn kinase induces synaptic and cognitive impairments in a transgenic mouse model of Alzheimer's disease. *J Neurosci* 25:9694–9703.
- Srivastava RA, Jain JC (2002) Scavenger receptor class B type I expression and elemental analysis in cerebellum and parietal cortex regions of the Alzheimer's disease brain. *J Neurol Sci* 196:45–52.
- Zamze S, et al. (2002) Recognition of bacterial capsular polysaccharides and lipopolysaccharides by the macrophage mannose receptor. *J Biol Chem* 277:41613–41623.
- Kim WK, et al. (2006) CD163 identifies perivascular macrophages in normal and viral encephalitic brains and potential precursors to perivascular macrophages in blood. *Am J Pathol* 168:822–834.
- Broadbent NJ, Squire LR, Clark RE (2004) Spatial memory, recognition memory, and the hippocampus. *Proc Natl Acad Sci USA* 101:14515–14520.
- Morris RG, Garrud P, Rawlins JN, O'Keefe J (1982) Place navigation impaired in rats with hippocampal lesions. *Nature* 297:681–683.
- Hickey WF, Kimura H (1988) Perivascular microglial cells of the CNS are bone marrow-derived and present antigen in vivo. *Science* 239:290–292.
- Nicolakakis N, et al. (2008) Complete rescue of cerebrovascular function in aged Alzheimer's disease transgenic mice by antioxidants and pioglitazone, a peroxisome proliferator-activated receptor  $\gamma$  agonist. *J Neurosci* 28:9287–9296.
- Wyss-Coray T, et al. (2003) Adult mouse astrocytes degrade amyloid- $\beta$  in vitro and in situ. *Nat Med* 9:453–457.
- Van Eck M, et al. (2007) Increased oxidative stress in scavenger receptor BI knockout mice with dysfunctional HDL. *Arterioscler Thromb Vasc Biol* 27:2413–2419.
- Tong XK, et al. (2009) Simvastatin improves cerebrovascular function and counters soluble amyloid- $\beta$ , inflammation and oxidative stress in aged APP mice. *Neurobiol Dis* 35:406–414.
- Higgins GA, Jacobsen H (2003) Transgenic mouse models of Alzheimer's disease: Phenotype and application. *Behav Pharmacol* 14:419–438.
- Chang EH, Rigotti A, Huerta PT (2009) Age-related influence of the HDL receptor SR-BI on synaptic plasticity and cognition. *Neurobiol Aging* 30:407–419.
- Huang F, et al. (1999) Elimination of the class A scavenger receptor does not affect amyloid plaque formation or neurodegeneration in transgenic mice expressing human amyloid protein precursors. *Am J Pathol* 155:1741–1747.
- Scholtzova H, et al. (2009) Induction of Toll-like receptor 9 signaling as a method for ameliorating Alzheimer's disease-related pathology. *J Neurosci* 29:1846–1854.
- Han J, et al. (2004) Functional interplay between the macrophage scavenger receptor class B type I and pitavastatin (NK-104). *Circulation* 110:3472–3479.
- Zhao SP, Wu ZH, Hong SC, Ye HJ, Wu J (2006) Effect of atorvastatin on SR-BI expression and HDL-induced cholesterol efflux in adipocytes of hypercholesterolemic rabbits. *Clin Chim Acta* 365:119–124.
- Fragkouli A, et al. (2005) Loss of forebrain cholinergic neurons and impairment in spatial learning and memory in LHX7-deficient mice. *Eur J Neurosci* 21:2923–2938.